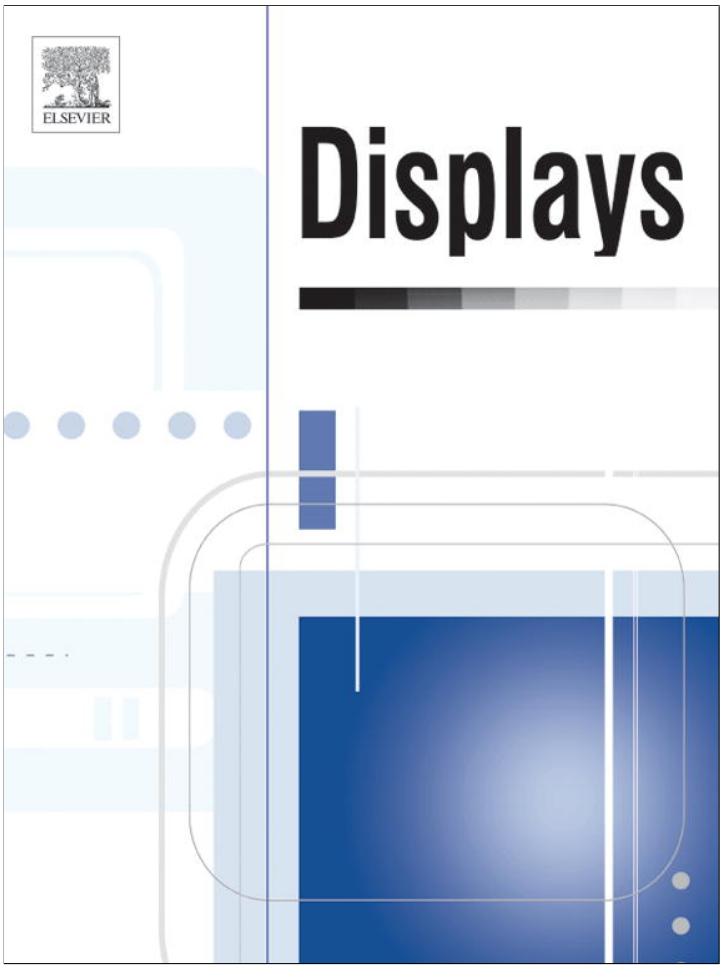

(This is a sample cover image for this issue. The actual cover is not yet available at this time.)

Displays 33 (2012) 136–141

Contents lists available at SciVerse ScienceDirect

Displays

journal homepage: www.elsevier.com/locate/displa

Reduction of spatially non-uniform 3D crosstalk for stereoscopic display using shutter glasses

HyungKi Hong *

Department of Visual Optics, Seoul National University of Science and Technology, Nowon-gu, Seoul, Republic of Korea

ARTICLE INFO

Article history:
Received 20 October 2011
Received in revised form 17 May 2012
Accepted 28 May 2012
Available online 4 June 2012

Keywords:
3 Dimensional display
Stereoscopic display
3D crosstalk
Ghost
Shutter glass

ABSTRACT

In 3D technology, when the image isolation between the left image and right image is incomplete, each eye can see not only wanted image but also unwanted image as well. And for some types of 3D technology, this leakage of the unwanted image is not spatially uniform. In making this leakage less noticeable by the modification of the 3D image data, one value of the modification condition can make the leakage smaller at one position but larger at other positions of the 3D display due to this non-uniformity. When the modification conditions dependent on the display positions are determined and applied to the image data, the leakage is observed to reduce at all the positions of the 3D display.

1. Introduction

Principle of 3D and various 3D technologies had been known for a long time [1,2]. Nowadays, 3D technologies become popular not only in 3D theater but also for the various applications such as TV, monitor [3].

When the image isolation between the left image and right image is incomplete in 3D display, the left eye of the user can see not only the left image but also the weak right image and vice versa. For example when the left and right images with non-zero binocular disparity of Fig. 1a are displayed, the luminance difference occurs at the region where the binocular disparity exist as illustrated in Fig. 1b. Such an image artifact is generally used to determine the image quality of 3D display. And this artifact is characterized by 3D crosstalk which is defined as the ratio of the unwanted image leakage to the wanted image [4].

Reduction of 3D crosstalk by the modification of the image data had been reported to be effective. Fig. 1c and d shows the schematic concept of 3D crosstalk reduction. Once leakage or 3D crosstalk is measured, original image data is modified such that sum of the luminance by the modified image data and the leakage becomes the original image data [5,6].

For some type of 3D technologies, 3D crosstalk had been reported to be spatially non-uniform due to the factors such as the signal driving scheme and the directional dependence [7,8]. If spatial non-uniformity of 3D crosstalk is not negligible, the conditions for 3D crosstalk reduction need to be determined in consideration of this non-uniformity.

In this paper, the spatial distribution of 3D crosstalk characteristic is determined through the observation of test image data of the spatial periodic pattern. From this, the conditions for 3D crosstalk reduction are separately determined for the different positions on the imaging display. Finally, the 3D crosstalk for the modified test image is compared with that of the original test image to confirm the usefulness of this approach.

2. Method

2.1. Phenomenon of non-uniformity

Spatial distribution of 3D crosstalk was investigated for stereoscopic 3D using Shutter glasses (SG 3D). 3D system for the experiment consists of Shutter glass (Nvidia 3D vision), 120 Hz monitor, PC equipped with Geforce GTX460 graphic card [9]. For the experiment, LCD monitor of Twisted Nematic (TN) LC mode, the diagonal size of 22 in. and the total pixel number of 1680 by 1050 was used (ViewSonic VX2268WM) which is compatible with the shutter glass of Nvidia 3D vision. To display the test image data on the 3D display, 3D photo viewer software of Nvidia was used which controls the synchronization of 3D signal for 3D monitor and the shutter glasses.

Test image data of Fig. 2 that consists of white and black signal was used as the 3D input image data. Black bars are repeated with the period of $W/9$. The binocular disparity of the black bars between the left and the right eye is $W/60$.

* Tel.: +82 19 345 7452; fax: +82 02 971 2852.
E-mail address: hyungki.hong@snut.ac.kr

0141-9382/$ - see front matter © 2012 Elsevier B.V. All rights reserved.
http://dx.doi.org/10.1016/j.displa.2012.05.003

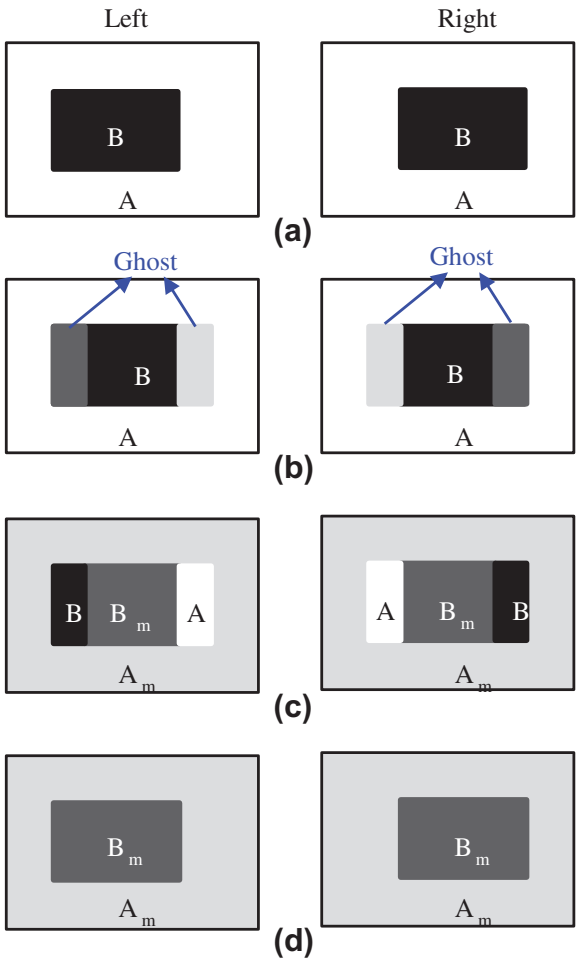

Fig. 1. Scheme of 3D crosstalk reduction by the modification of the image data. (a) Original image data for the left and the right eye. (b) Images observed by the left and the right eye through eyeglasses when the original images are displayed. (c) Image data modified to reduce 3D crosstalk. (d) Images observed by the left and the right eye through eyeglass when the modified image data are used.

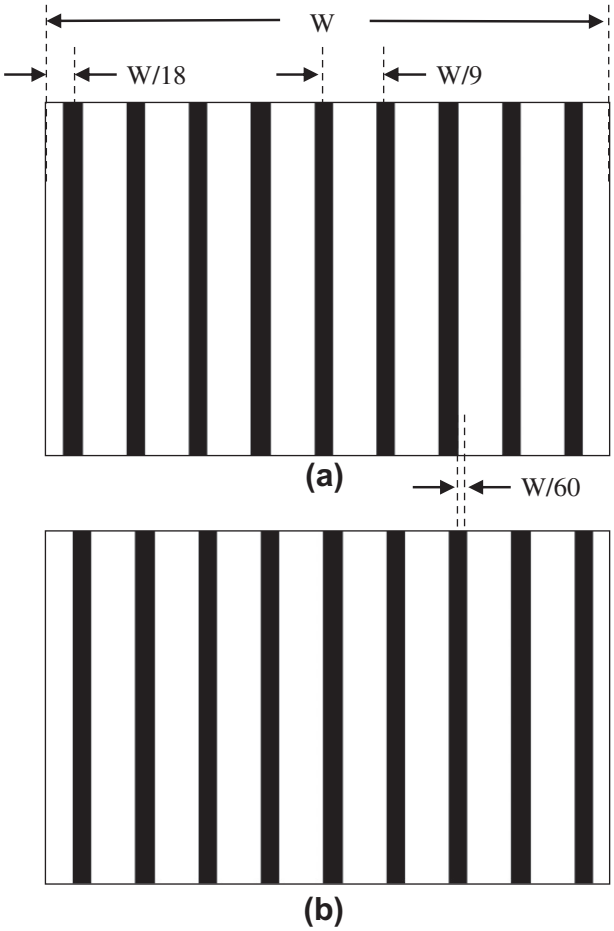

Fig. 2. Test image data of the repeated bar patterns for 3D crosstalk observation for (a) the left eye and (b) the right eye. Black bars are repeated with the period of $W/9$ on the white background. W represents the width of the test image data or the 3D display. The binocular disparity between bars of the left and the right image data is $W/60$.

To capture the image that is observed by one eye, digital camera (Canon EOS 500D) was used. Digital photo image is saved as 24 bit JPG image. It was placed at the distance of 80 cm from the 3D display, perpendicular to the center of the 3D display as illustrated in Fig. 3a. Right side of the operating shutter glasses were placed in front of digital camera.

Fig. 3b shows the photo captured through right side of the shutter glass when the test image data of Fig. 2 was displayed on the 3D display. Experiment was performed 30 min after 3D display is turned on. At the left side of each black bar, weak vertical patterns can be observed. These correspond to the test image data for the left eye. This leakage of the unwanted image is defined as ghost artifact in this paper. The intensity of this ghost artifact is known to increase as the 3D crosstalk increases [4]. Fig. 3b shows the non-negligible change of the ghost artifact along the vertical direction and the relatively negligible change along the horizontal direction. Fig. 3c shows the gray level along the cross-section S_1–S_2 of the digital image of the captured photo. The maximum gray level of the photo is normalized from 255 to 1. Positions of the cross section are represented as line S_1–S_2 in Fig. 3b. Step-like change of gray levels corresponding to the ghost artifact can be observed beside the left side of the each region which corresponds to the input signal of black bar.

The vertical non-uniformity of this SG 3D system can be attributed to the driving scheme of LCD where each new image is vertically updated line by line sequentially from the top line to the bottom line during each frame [4]. Fig. 3 shows that the intensity of the ghost artifact and 3D crosstalk are not spatially uniform for the SG 3D used in the experiment. Therefore, in applying the concept of 3D crosstalk reduction to this SG 3D, the effect of this non-uniformity needs to be investigated.

2.2. Experimental set-up for 3D crosstalk reduction

The intensities of the ghost artifacts of Fig. 3 do not shows any abrupt change at any specific positions. Hence, if the image modification conditions for 3D crosstalk reductions are determined at the finite number of positions of the 3D display, it is expected that the image modification condition at any position can be determined by the interpolation.

While Figs. 2 and 3 show the ghost artifact for the case of the black and the white signal, ghost artifacts between other gray levels needs to be investigated. Test image data of repeated boxes of Fig. 4 is used which consist of two different gray levels. Gray levels of 0, 63, 127, 191 and 255 are considered. Input signal for the white and the black correspond to the gray levels of $A = 255$ and $B = 0$. In Fig. 4, 9 by 9 boxes are repeated vertically with the period of $H/9$ and horizontally with the period of $W/9$. P_{nl} represent the location of each box on the 3D display where the first and the second subscripts are related to the vertical and the horizontal positions. The binocular disparity of boxes between the left and the right images

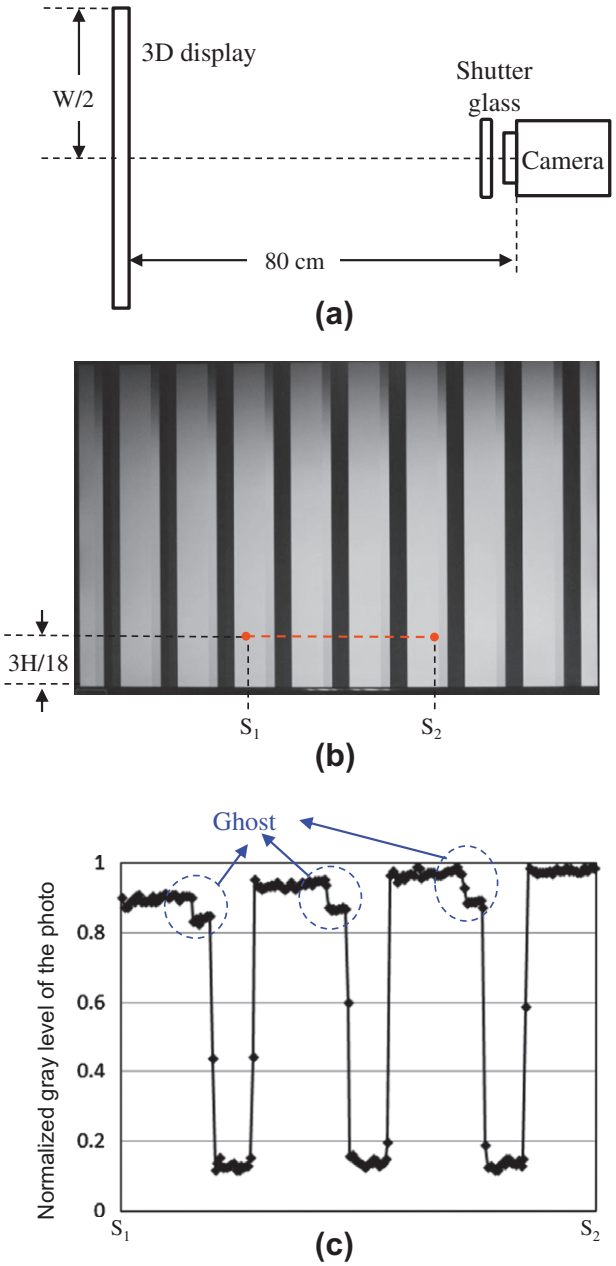

Fig. 3. (a) Top view of the photo-capturing system. Digital camera is placed perpendicular to the 3D display. (b) Photo captured through the right side of eyeglass when the test image data of Fig. 2 were displayed on the 3D display (c) Normalized gray level of the captured photo along the line S_1–S_2. Horizontal axis represents the positions between S_1 and S_2. Vertical axis represents the normalized gray level of photo.

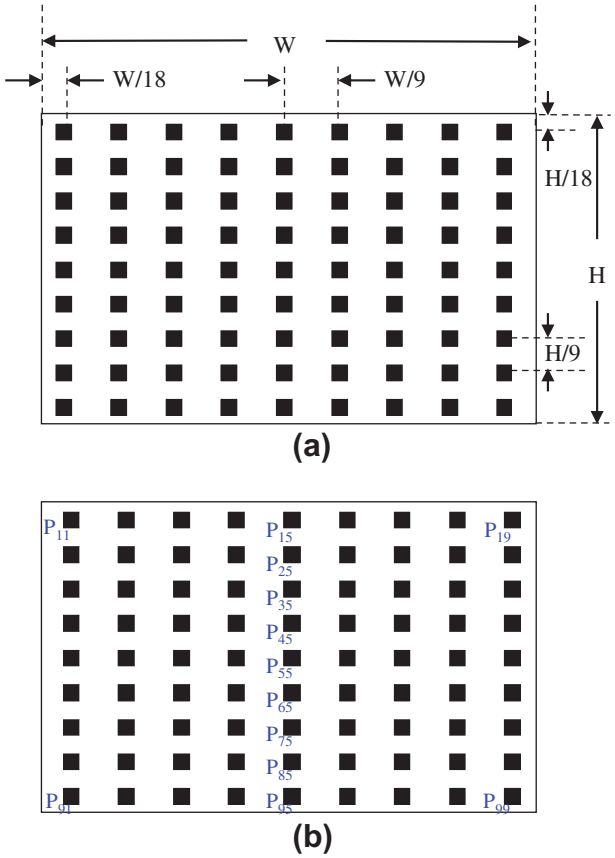

Fig. 4. Test image data of the repeated box patterns for 3D crosstalk observation for (a) the left eye and (b) the right eye. The boxes are placed horizontally with the period of $W/18$ and vertically with the period of $H/18$. W and H represent the width and the height of the test image data or the 3D display. The binocular disparity between the boxes of the left and the right image data is $W/60$. Boxes are represented as P_{nl} and box of P_{55} is placed at the center of 3D display. The gray levels of the background and the box patterns are represented as A and B which are one of 0, 63, 127, 191, 255 gray levels.

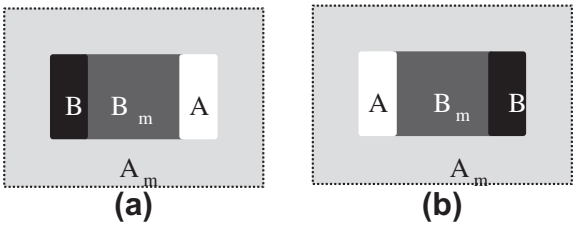

Fig. 5. Scheme of the modification of the image data of box patterns consisting of gray levels A and B for (a) the left eye and (b) the right eye. Gray levels for A_m and B_m are modified from gray levels A and B.

is $W/60$. Test image data of the repeated patterns are selected to observe the spatial uniformity of 3D crosstalk.

SG 3D system and photo-capturing system described in Section 2.1 was also used for the experiment. When this test image data is used, ghost artifact will appear around box pattern if 3D crosstalk is not negligible.

To find the condition of 3D crosstalk reduction, the image data are modified as illustrated in Fig. 5. In the modified image data, gray levels of A_m and B_m in the test image data are adjusted from gray level A and B by the step of four gray. As the each modified image is displayed on the 3D display, intensity of ghost artifact is observed. And the modification condition where ghost artifact is least observed is determined for each box pattern located at the different position of the 3D display. As the intensity of the ghost artifact depends on the 3D crosstalk, decrease of the ghost artifact will result in the reduction of 3D crosstalk as well.

3. Result and analysis

Fig. 6 shows the photo captured through the right side of shutter glass when test image data of box pattern of Fig. 4 is displayed with gray levels of $A = 255$ and $B = 0$. In Fig. 6, ghost artifact show the trend of the increase from the center of the 3D display along the vertical direction and the relatively negligible change along

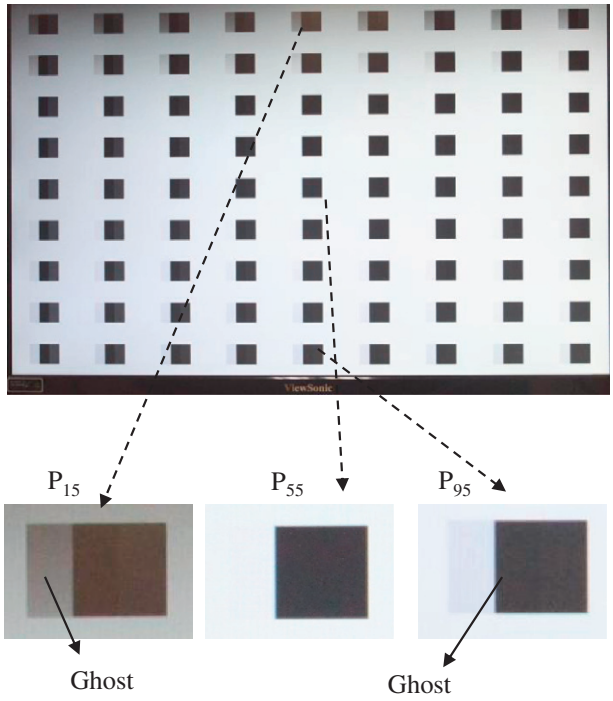

Fig. 6. Photo captured through the right side of eyeglass when the test image data of Fig. 4 at $A = 255$ and $B = 0$ are displayed on the 3D display. Enlarged images around box pattern P_{15} and P_{95} show the ghost artifact where box patterns for the left eye leaked. Enlarged image around box pattern P_{55} shows no ghost artifact.

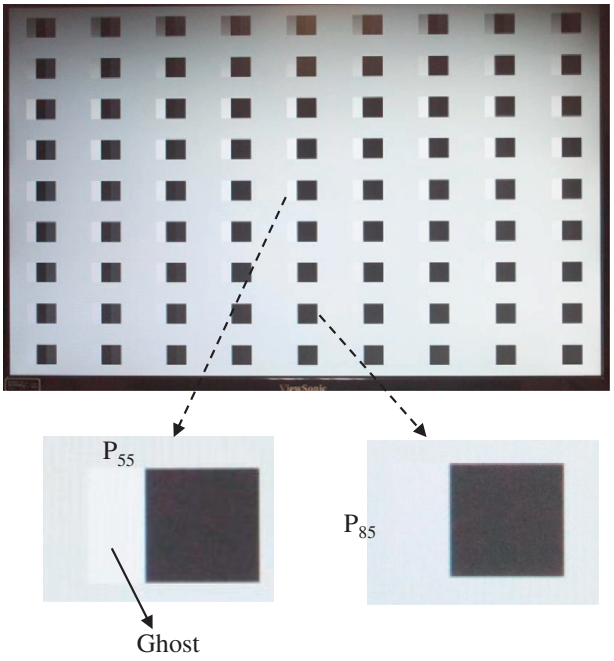

Fig. 7. Photo captured through the right side of eyeglass when the modified test image data of Fig. 5 at $A = 255$, $B = 0$, $A_m = 183$ and $B_m = 0$ are displayed on the 3D display. Enlarged image around the box pattern P_{85} shows little ghost artifact. Enlarged image around box pattern P_{55} and the upper side of the captured photo shows the stronger ghost artifact compared with that of Fig. 6.

the horizontal direction similar to Fig. 3. Enlarged image around the box pattern of P_{55} shows that ghost artifact is less noticeable at the center of the 3D display. Enlarged images around the box pattern of P_{15} or P_{95} show stronger ghost artifact compared with that around the center position. Also intensity of the ghost artifact is not symmetric along the vertical direction.

As the non-uniformity along the horizontal direction is not noticeable, conditions of image modification were determined only at the nine positions of P_{15}, P_{25}, ... P_{85}, P_{95} along the vertical direction, following the procedure described in Section 3.

Conditions of A_m and B_m where the ghost artifact becomes least noticeable are not the same for the nine points along the vertical direction. These are determined respectively by the visual observation as the A_m and B_m values for the modified image data are adjusted. Modification conditions for these nine points are listed in Table 1. Values of B_m remain zero for the gray levels of $A = 255$ and $B = 0$ in case of this 3D system.

Fig. 7 shows an example of the captured photo when the modified test image data of $A_m = 187$ and $B_m = 0$ is used. Enlarged image around the box pattern of P_{85} shows that ghost artifact is not noticeable, but the ghost artifact at the center and the upper side of the 3D display are more noticeable compared with Fig. 6. Therefore, this modification condition of $A_m = 187$ and $B_m = 0$ is not effective for all the positions of 3D display.

From the A_m values of Table 1, A_m value at the each vertical pixel position of the image data is determined using Least-Squares Fitting technique, where 5th – degree polynomial is used. Fitting curve of A_m is illustrated in Fig. 8. The fitting curve is steeper at the upper side compared with the lower side of the image data. Fig. 9 shows the modified image data of the bar patterns where A_m value changes continuously according to the fitting curve of Fig. 8.

Photo captured through the right side of shutter glass is shown in Fig. 10a when the modified image data of Fig. 9 is used. Photo of Fig. 10a shows the weaker ghost artifact compared with that of Fig. 3. Fig. 10b shows the gray level of the digital image of the captured photo where the maximum gray level is normalized to one. Positions of the cross section are represented as line S_1–S_2 in Fig. 10a. The step-like change due to the ghost-artifact existed in

Table 1
A_m and B_m values which is determined when the ghost artifact is least noticeable at each position of box pattern along the vertical direction for the image data of box patterns consisting of gray levels $A = 255$ and $B = 0$.

Position	P_{15}	P_{25}	P_{35}	P_{45}	P_{55}	P_{65}	P_{75}	P_{85}	P_{95}
A_m	151	199	227	243	235	207	195	183	173
B_m	0	0	0	0	0	0	0	0	0

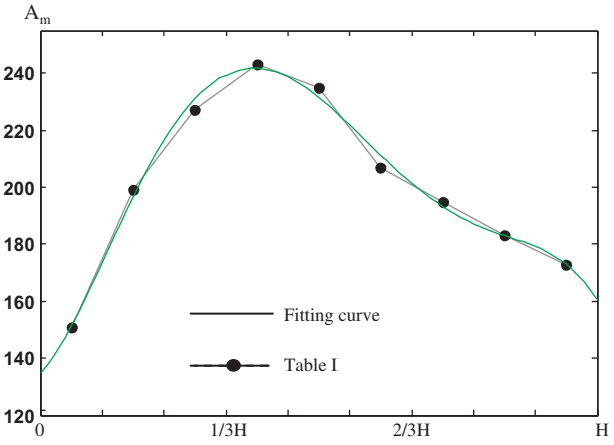

Fig. 8. Fitting curve of A_m using the data of Table 1 for the test image data of Fig. 4 at $A = 255$ and $B = 0$. Horizontal axis represents the vertical positions of the 3D display where 0 and H correspond to the top and the bottom positions of the 3D display. Vertical axis represents A_m for the modified image data.

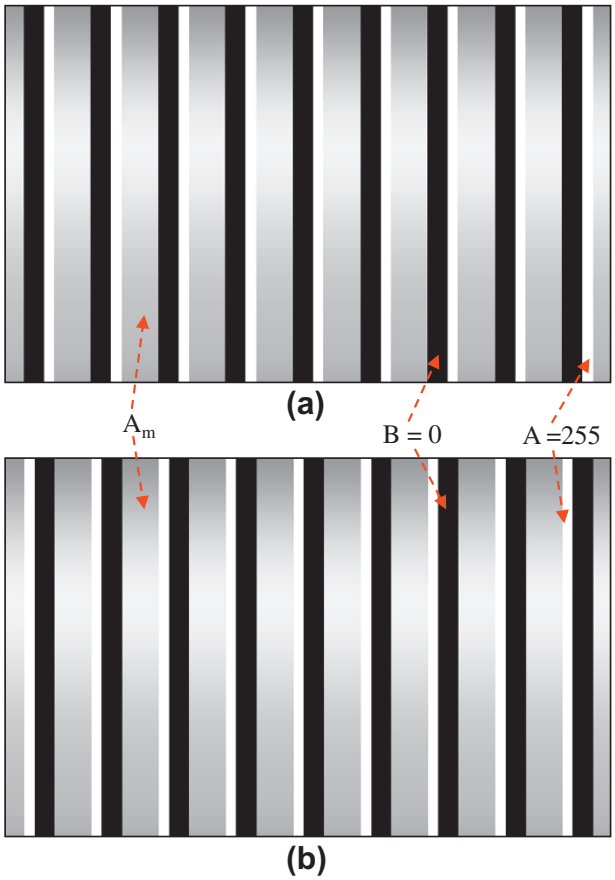

Fig. 9. Modified image data of the bar patterns of Fig. 2 for (a) the left and (b) the right eye. A_m of image data is modified according to the fitting curve of Fig. 8. *A* and *B* correspond to the gray levels for white and black.

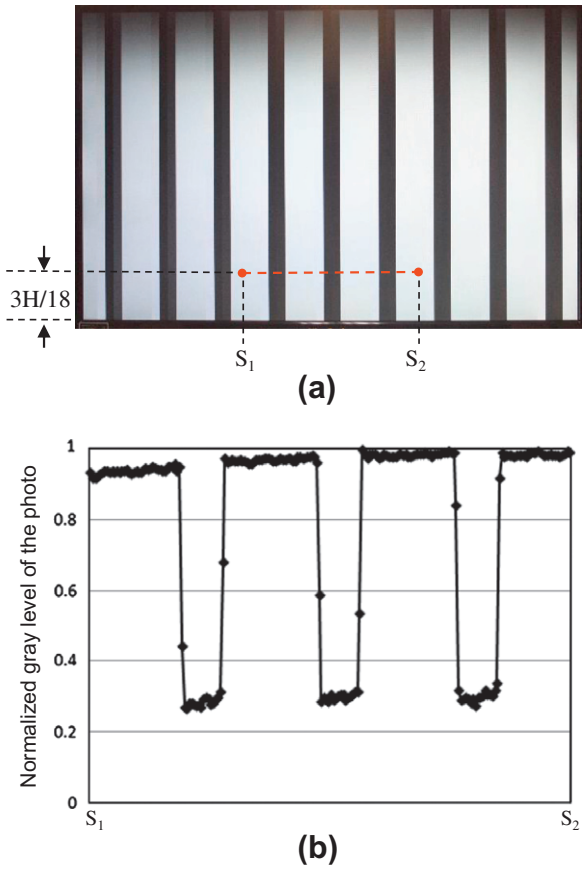

Fig. 10. (a) Photo captured through the right side of eyeglass when the modified test image data of Fig. 9 are displayed on the 3D display. (b) Normalized gray level of the captured photo along the line S1–S2. Horizontal axis represents the positions between S1 and S2. Vertical axis represents the normalized gray level of photo.

Fig. 3c where the non-modified image data is used. But in Fig. 10b, these step-like change due to the ghost-artifact does not exist.

Procedure described in the above for the test image data of the black and white can be applied to determine the condition of 3D crosstalk reduction for other gray levels. For this, the gray levels of the background and the box patterns in Fig. 4 are selected as $A = 63, 127, 191$ and $B = 0, 63$. Each test image that consist of the combination of *A* and *B*, was displayed on the 3D sample and A_m and B_m are determined which reduce 3D crosstalk in consideration of the spatial non-uniformity. When these test images are displayed on the 3D sample, the observed ghost artifacts show the trend similar to that of Fig. 6 where the ghost artifacts increase from the center of the 3D display along the vertical direction and relatively change little along the horizontal direction. So A_m and B_m are determined at the vertical nine positions of P_{15}, P_{25}, ... P_{85}, P_{95}. Similar to the case of the black and white, ghost artifact are observed to be stronger near the boundary along the vertical direction. Fig. 11 illustrates the results for the gray level of $B = 0$. Change of A–A_m can reduce the observed ghost artifact while B_m was kept the same as $B = 0$. A_m deviates from *A* more at the regions of the strong ghost artifacts. Fig. 12 illustrates the determined A_m and B_m for the gray level of $B = 63$. Ghost artifact can occur inside the box pattern as well as outside the box pattern. When the value of A_m decreases from *A* by the step of four gray levels, the ghost artifact observed outside the box pattern is reduced. When B_m increases from *B* by the step of four gray levels, the ghost artifact observed inside the box pattern is reduced. As the ghost artifact observed outside the box pattern is more noticeable than the ghost artifact observed inside the box pattern, A_m was first determined

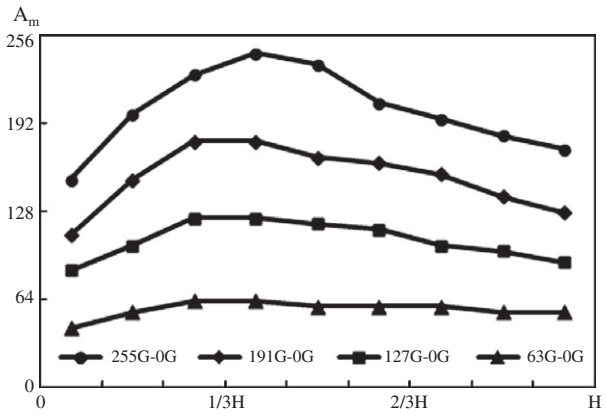

Fig. 11. Conditions of A_m for 3D crosstalk reduction determined from the image data of box patterns consisting of gray levels of $A = 63, 127, 191, 255$ and $B = 0$. B_m is fixed as zero. Horizontal axis represents the vertical positions of the 3D display where 0 and *H* correspond to the top and the bottom positions of the 3D display. Vertical axis represents gray levels of A_m for the modified image data. List of number inside the graph represent the gray levels for *A* and *B*.

and then B_m was determined. Without the image modification, the ghost artifact at $3H/9$ and $4H/9$ are least noticeable. So A–A_m and B_m–B are smaller at these positions.

Once conditions of A_m and B_m are determined with respect to the specific spatial positions and the specific gray levels, conditions of A_m and B_m for the intermediate state can be derived as illustrated in the example of Figs. 8 and 9 for the gray levels of 255 and 0.

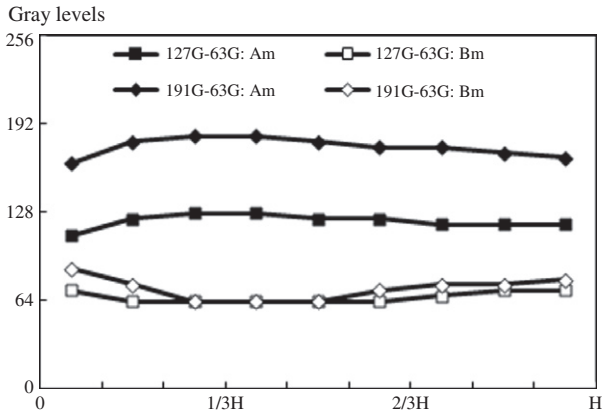

Fig. 12. Conditions of A_m and B_m for 3D crosstalk reduction determined from the image data of box patterns consisting of gray levels of $A = 127$, 191 and $B = 63$. Horizontal axis represents the vertical positions of the 3D display where 0 and H correspond to the top and the bottom positions of the 3D display. Vertical axis represents gray levels of A_m and B_m for the modified image data. List of number inside the graph represent the gray levels for A and B.

4. Conclusion

Ghost artifact due to the incomplete isolation between the left and the right eyes is observed to be non-uniform along the vertical direction for 3D display using the shutter glass and LCD monitor of TN mode. As the ghost artifact or the 3D crosstalk is not spatially uniform along the vertical direction, 3D crosstalk reduction by the modification of the image data is not effective for all the positions of the 3D display when modification condition of one value is used. Modification conditions to reduce the 3D crosstalk were determined at the vertical nine positions on the 3D display between the gray levels of 0, 63, 127, 191 and 255. When modification conditions were interpolated from these determined conditions, ghost artifact, that is, 3D crosstalk was observed to decrease for all the positions of 3D display.

The modification condition is determined for the stereoscopic system consisting of 3D display and the shutter glasses. Hence, the replacement of 3D display or the shutter glass in the stereoscopic system by other devices, may affect the modification condition, though this does not affect the described procedure determining the modification condition.

If data modification is done disregarding the spatial non-uniformity, this can even cause the increase of the 3D crosstalk at some positions as shown in Fig. 7. On the other hand, data modification in consideration of the spatial non-uniformity can reduce the spatial 3D crosstalk, but this method is more complex and needs large amount of data compared with the former. Also, this modification of the image data can cause the gradual non-uniformity of the luminance distribution along the vertical direction. Hence, the usefulness of the spatial non-uniformity should be considered regarding how strongly the performance of the stereoscopic system shows the spatially non-uniform behavior.

Acknowledgment

This study was financially supported by Seoul National University of Science & Technology. Author thanks Seoul National University of Science and Technology for the support of this study.

References

[1] B. Javidi, F. Okano, Three-Dimensional Television, Video and Display Technologies, Springer Press, New York, 2002.
[2] T. Kawai, 3D displays and applications, Displays 23 (2002) 49–56.
[3] The Illustrated 3D Movie List, <http://www.3dmovielist.com> (accessed October 2011).
[4] A.J. Woods, How are crosstalk ghosting defined in the stereoscopic literature?, Proceedings of SPIE Stereoscopic Displays and Applications 7863 (2011) 78630Z-1–78630Z-12.
[5] J.S. Lipscomb, W.L. Wooten, Reducing crosstalk between stereoscopic views, Proceedings of SPIE Stereoscopic Displays and Virtual Reality Systems 2177 (1994) 92–96.
[6] J. Konrad, Cancellation of image crosstalk in time-sequential displays of stereoscopic video, IEEE Transactions on Image Processing 9 (2000) 897–908.
[7] A.J. Woods, A. Sehic, The compatibility of LCD TVs with time-sequential stereoscopic 3D visualization, Proceedings of SPIE Stereoscopic Displays and Applications 7237 (2009).
[8] H.K. Hong, K.H. Lim, J.H. Kim, S.H. Park, H.S. Shin, D.G. Lee, H.H. Shin, Angular dependence of the performance of stereoscopic liquid-crystal-display (LCD) television using shutter glasses (SG), Journal of the Society of Information Display 19 (2011) 287–294.
[9] Nvidia 3D Vision, <www.nvidia.com/object/3d-vision-main> (accessed October 2011).